# The Crystal Structure of $Ti_4O_7$, a Member of the Homologous Series $Ti_nO_{2n-1}$*

M. MAREZIO AND P. D. DERNIER

*Bell Telephone Laboratories, Incorporated*
*Murray Hill, New Jersey*

$Ti_4O_7$, a member of the homologous series $Ti_nO_{2n-1}$, is triclinic with four formula units per unit cell where $a = 5.600 \pm 0.002$ Å, $b = 7.133 \pm 0.003$ Å, $c = 12.466 \pm 0.005$ Å, $\alpha = 95.05 \pm 0.01°$, $\beta = 95.17 \pm 0.01°$, and $\gamma = 108.71 \pm 0.02°$, and the calculated density is 4.32 g/cm³. The positional and anisotropic thermal parameters have been refined by the least-squares method based on 1104 structure factors. The final conventional $R$ index is 0.025. The structure consists of rutile-like layers of $TiO_6$ octahedra extending indefinitely in the $a$–$b$ plane and four octahedra thick along the $c$ axis. The sharing of octahedral faces, edges, and corners between rutile layers is similar to that which occurs in the corundum structure. The overall average Ti–O and O–O distances are 2.012 and 2.826 Å, respectively. The average Ti–O distances for individual octahedra range from 2.004 to 2.022 Å indicating that the titanium charge is very nearly equally distributed among the rutile and corundum-like sites. The average Ti–Ti distances within a rutile layer are 2.972 and 3.576 Å across a shared octahedral edge and corner, respectively, whereas the average distances across a shared face and edge in the corundum-like layer are 2.815 and 3.149 Å, respectively.

## Introduction

The concept of the homologous series in inorganic chemistry was introduced by Magnéli and his school, who studied several molybdenum oxides and found common structural principles among them. Subsequently, other homologous series were found in many transition metal oxide systems. An important one was found in the titanium–oxygen system, $Ti_nO_{2n-1}$ ($n = 4$, 5, ...) (*1–3*). S. Andersson and Jahnberg (*4*) were able to fully index the powder patterns of each member of this series on triclinic cells by recognizing in each pattern a rutile-like substructure. They were also able to outline the arrangements of these oxides by solving the structure of the second member of the series, $Ti_5O_9$. The arrangement of each member of the series may be described as containing slabs of rutile, extending infinitely in two dimensions and having a finite width

of $n$ octahedra in the third direction. The octahedra at the ends of each rutile block share faces, edges, and corners with the corresponding ones of the next rutile block. This sharing is similar to the one occurring in the corundum structure. The oxide $Ti_3O_5$ has been reported as dimorphic with a transition temperature of 120°C. Both phases have monoclinic symmetry, but neither of which has the arrangement of the succeeding members of the series (*5*).

Bartholomew and Frankl (*6*) recently reported an increase of about $10^5$ in the electrical resistivity of $Ti_4O_7$ at two closely spaced temperatures, ~150 and 125°K. D. B. McWhan, J. P. Remeika, and these authors have also observed a discontinuous change in lattice parameters of $Ti_4O_7$ powder at approximately 150°K (*7*). Many of the transition metal oxides with less than two $d$ electrons per transition metal ion show induced metal to insulator transitions. A large number of theoretical models have been proposed in order to explain these transitions. Since it is necessary to know very accurate interatomic distances in order to understand the driving mechanism for these transitions, this paper reports the determination and refinement of the crystal structure of the first triclinic member of the homologous series $Ti_nO_{2n-1}$.

## Crystal Data

The single crystals used in this investigation were kindly supplied by R. F. Bartholomew and W. B. White of the Materials Research Laboratory of the Pennsylvania State University. The crystal growth procedure was reported by these authors elsewhere (8).

A single crystal having the shape of a small prism was oriented on a precession camera, with the $b$ axis as the precessing axis. Every spot which appeared on the long exposure photographs taken with Mo $K_\alpha$ radiation could be indexed on the triclinic cell given by Andersson and Jahnberg (4):

$$a = 5.600 \pm 0.002 \text{ Å} \quad \alpha = 95.05 \pm 0.01°$$
$$b = 7.133 \pm 0.003 \text{ Å} \quad \beta = 95.17 \pm 0.01°$$
$$c = 12.466 \pm 0.005 \text{ Å} \quad \gamma = 108.71 \pm 0.02°$$

These values were obtained by applying the least-squares method to the $\sin^2 \theta$'s reported by Andersson and Jahnberg. The reduced cell, determined by the method described by Santoro and Mighell (9), proved that the cell suggested by Andersson and Jahnberg is a primitive cell and that the lattice symmetry of $Ti_4O_7$ is indeed triclinic. The unit cell contains four formula units, the space group is either $P1$ or $P\bar{1}$ and the calculated density is 4.32 g/cm³.

## Experimental

The intensity measurements were taken with a paper-tape controlled, fully automatic General Electric XRD-5 X-ray diffractometer. An 8° take-off angle was used along with a scintillation counter, decade scalar, and single Zr-filtered Mo $K_\alpha$ radiation. The integrated intensities were obtained by use of the stationary crystal stationary counter technique. The specimen was a sphere of radius $R = 0.011$ cm. All reflections in the upper hemisphere of reciprocal space in the region $2\theta \leqslant 67°$ were measured. The background was measured on each side of the peak at 2° off the peak itself and the average was subtracted from the peak height. A standard reflection was also monitored so as to keep a running check on crystal orientation. A total of 3693 reflections were measured, of which 1241 were independent and well above background. The Lorentz, polarization, and absorption corrections were applied in order to convert the integrated intensities into structure factors. The absorption coefficient for Mo $K_\alpha$ was taken as 68.09 cm⁻¹; for the sphere used $\mu R = 0.749$.

## Solution of the Structure

Since the structure could not be refined by using the positional parameters given by Andersson and

Jahnberg (4), a three-dimensional Patterson synthesis was computed using the program Four written by Fritchie (10) and modified by L. Guggenberger and P. B. Jamieson. The squares of the 1241 observed structure factors on an arbitrary scale were the input terms. Since there was no difference between $F_{hkl}$ and $F_{\overline{hkl}}$ their average was used and the structure was solved by assuming the centrosymmetric space group $P\bar{1}$. All major peaks in the Patterson synthesis could be explained by placing the eight titanium atoms of the asymmetric unit in the same positions given by Andersson and Jahnberg. Structure factors based on these coordinates, assuming isotropic temperature factors of 0.4 Å (2), correspond to $R = \Sigma ||F_o| - |F_c||/\Sigma|F_o| = 0.47$ which reduced to 0.27 after three cycles of refinement with the least-squares program ORFLS (11). The $f$-curve for neutral titanium and later for neutral oxygen given by Cromer and Waber (12) were used together with the values of $\Delta f'$ and $\Delta f''$ for Ti reported by Cromer (13). A three-dimensional Fourier synthesis, computed with the signs of the eight titanium atoms, gave the positions of the 14 oxygen atoms. However, for each oxygen position $(x,y,z)$ there was also a spurious one at $(x,\frac{1}{2}+y,z)$ so that in the Fourier there were two sets of 14 oxygen atoms. This can be explained by the fact that among the eight titanium atoms there are two sets of four, one at $(x,y,z)$ and the other at approximately $(x,\frac{1}{2}+y,z)$. Since the signs of the structure factors for the first Fourier were those of the titanium contributions only, the same relationship held for the oxygen atoms. It was readily seen which set of oxygen parameters was the correct one. A three-dimensional Fourier computed with the signs of the eight titanium and 14 oxygen atoms did not show any spurious peaks.

The symmetry of the substructure is much higher than triclinic and therefore each titanium atom $(x,y,z)$ of the triclinic cell has three pseudoequivalent ones at $(x,\frac{1}{2}+y,z)$, $(x,y,\frac{1}{2}+z)$ and $(x,\frac{1}{2}+y,\frac{1}{2}+z)$, whereas each oxygen has only pseudoequivalent atom at $(x,\frac{1}{2}+y,\frac{1}{2}+z)$. These relationships prevented a complete least-squares refinement of the positional parameters. They caused very strong correlations between parameters belonging to pseudorelated atoms. It was decided to carry out the refinement in two steps using the least-squares program written by C. T. Prewitt (14). The function minimized was $\Sigma w ||F_o| - |F_c||^2$ where $w = 1/\sigma^2$, $\sigma = 2.5$ when $|F_o| \leqslant 25$, and $\sigma = 0.1|F_o|$ when $|F_o| > 25$, for all reflections except those for which $k + l = 2n + 1$. These reflections were all very weak, barely twice the background and, therefore, less

## TABLE I

### FINAL POSITIONAL AND THERMAL PARAMETERS

|        | $x$       | $y$       | $z$       | $B$ (Å²) |
|--------|-----------|-----------|-----------|----------|
| Ti(1)  | 0.2159(2) | 0.1526(1) | 0.0629(1) | 0.42(2)  |
| Ti(2)  | 0.2186(2) | 0.6528(1) | 0.0663(1) | 0.42(2)  |
| Ti(3)  | 0.2165(1) | 0.6530(1) | 0.5628(1) | 0.50(2)  |
| Ti(4)  | 0.2185(2) | 0.1524(1) | 0.5661(1) | 0.45(2)  |
| Ti(5)  | 0.6836(1) | 0.4401(1) | 0.2013(1) | 0.42(2)  |
| Ti(6)  | 0.6881(1) | 0.9422(1) | 0.2013(1) | 0.42(2)  |
| Ti(7)  | 0.6833(1) | 0.9399(1) | 0.7011(1) | 0.45(2)  |
| Ti(8)  | 0.6891(1) | 0.4425(1) | 0.7014(1) | 0.51(2)  |
| O(1)   | 0.1042(6) | 0.8637(5) | 0.0180(3) | 0.52(5)  |
| O(2)   | 0.5832(6) | 0.7974(5) | 0.0562(3) | 0.48(4)  |
| O(3)   | 0.8473(6) | 0.4930(5) | 0.0778(3) | 0.54(5)  |
| O(4)   | 0.3354(6) | 0.4404(5) | 0.1396(3) | 0.52(4)  |
| O(5)   | 0.5314(6) | 0.1467(5) | 0.1666(3) | 0.56(5)  |
| O(6)   | 0.0400(6) | 0.0771(5) | 0.1994(3) | 0.54(4)  |
| O(7)   | 0.2964(6) | 0.7949(5) | 0.2258(3) | 0.49(5)  |
| O(8)   | 0.2928(6) | 0.2859(5) | 0.7220(2) | 0.49(4)  |
| O(9)   | 0.0350(5) | 0.5630(5) | 0.6969(3) | 0.39(5)  |
| O(10)  | 0.5221(5) | 0.6432(5) | 0.6613(2) | 0.41(4)  |
| O(11)  | 0.3209(6) | 0.9367(5) | 0.6377(3) | 0.43(4)  |
| O(12)  | 0.8641(5) | 0.9996(5) | 0.5845(2) | 0.54(5)  |
| O(13)  | 0.5907(6) | 0.2867(6) | 0.5595(3) | 0.53(4)  |
| O(14)  | 0.1105(6) | 0.3615(5) | 0.5119(3) | 0.58(5)  |

reliable. A $\sigma = 4.0$ was found to be appropriate for this type of reflections. Because of high background errors for those reflections for which $\sin\theta/\lambda \leqslant 0.25$, zero weight was assigned to the corresponding structure factors. This resulted in a final set of 1104 reflections, of which only 37 had $k + l = 2n + 1$. In the first step, the scale factor, the secondary extinction coefficient, the positional and isotropic thermal parameters of half of the asymmetric unit were varied for one cycle, namely Ti(1), Ti(2), Ti(5), Ti(6), and from O(1) through O(7), while the parameters corresponding to the other half were kept constant. In the second step, the positional and thermal parameters of Ti(3), Ti(4), Ti(7), Ti(8) and from O(8) through O(14) were varied together with the scale factor and the secondary extinction coefficient, while the values which were varied in the previous cycle were kept constant. The results of the final refinement which gave $R = 0.025$ and $wR = [\Sigma(w^{1/2}\Delta F)^2/\Sigma(w^{1/2}F_o)^2]^{1/2} = 0.044$ are shown in Table I. The table which shows the degree of agreement between observed and calculated structure factors is not included but is available on request.

In the last six cycles of refinement, anisotropic thermal parameters were introduced. This resulted in a smaller $R$ factor, 0.023 as against 0.025, indicating that the thermal motion is slightly anisotropic. However, the correlation between $B_{ij}$ of

pseudorelated atoms was extremely high and prevented complete convergence. Nevertheless the positional parameters did not change more than one standard deviation. It can be seen from Table I, where the final positional parameters are reported, that the pseudorelationship between $(x,y,z)$ and $(x,\frac{1}{2}+y,\frac{1}{2}+z)$ is almost exact for the titanium atoms, whereas it is not nearly as close for the oxygen atoms.

### Description of the Structure

The triclinic unit cell of $Ti_4O_7$ contains two rutile-like blocks of $TiO_6$ octahedra. These blocks extend indefinitely in the $a$–$b$ plane but they are only four octahedra thick along the $c$ axis. The orientation of the triclinic cell with respect to the rutile one is given by the following matrix $(4)$:

$$\begin{pmatrix} a_t \\ b_t \\ c_t \end{pmatrix} = \begin{pmatrix} 1 & 0 & \bar{1} \\ 1 & 1 & 1 \\ 1 & \bar{2} & 2 \end{pmatrix} \begin{pmatrix} a_r \\ a_r \\ c_r \end{pmatrix}$$

Figure 1 is a projection of the structure down the $a$ axis. The structure was mapped onto a cartesian coordinate system according to the equations:

$$X = u_1 + u_2 \cos\gamma + u_3 \cos\beta,$$
$$Y = u_2 \sin\gamma - u_3 \cos\alpha^* \sin\beta,$$
$$Z = u_3 \sin\alpha^* \sin\beta,$$

where $u_1$, $u_2$, and $u_3$ are the products of the fractional coordinates $x$, $y$, $z$ and the cell parameters, respectively. The $X$ direction is coincident with the $a$ axis, and the $b$–$c$ plane slopes down and away from the origin. Within the unit cell there is one complete rutile-like slab which is sandwiched between one-half of two adjacent slabs. The rutile $c$ axis runs roughly parallel with the shaded set of octahedra in Fig. 1. The layers of octahedra containing Ti atoms 5, 6, 7, and 8 have a corundum-like arrangement, which is more clearly illustrated in Fig. 2, where the idealized corundum structure is also shown for comparison. The break in the rutile-like structure along the triclinic $c$ axis is shown in the idealized drawing, Fig. 3, where the relative shift of titanium atoms is depicted. One layer of empty rutile sites is also shown in Fig. 1. It can be seen that the oxygen array in $Ti_4O_7$ is still h.c.p. as in both the rutile and corundum structures. One rutile unit cell is illustrated in Fig. 4. This cell when viewed along the $\langle 101 \rangle$ direction will give a portion of the rutile slab of Fig. 1.

The interatomic distances are reported in Tables II, III, and IV. These values and their standard
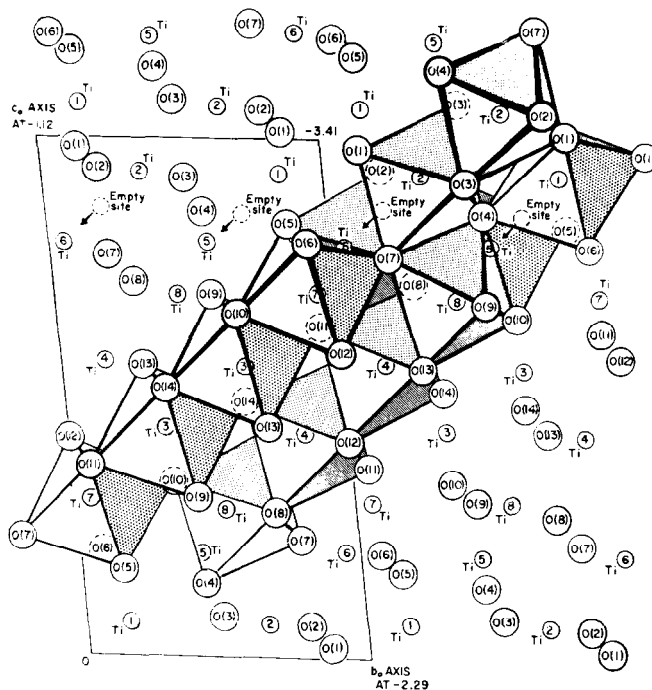
FIG. 1. A projection of the $Ti_4O_7$ structure down the triclinic $a$ axis. The shaded set of octahedra runs roughly parallel with the rutile $c$ axis.

deviations were calculated by the program ORFEE (15). The overall average Ti–O and O–O distances are 2.012 and 2.826 Å, respectively. Among the eight titanium atoms in the unit cell one can distinguish two types, one type includes Ti(1) through Ti(4) which are found inside the rutile block, and the second type includes Ti(5) through Ti(8) which are found at the ends of the rutile block. Within a rutile block, the oxygen octahedra share edges and corners just as they do in pure rutile. Between rutile blocks,
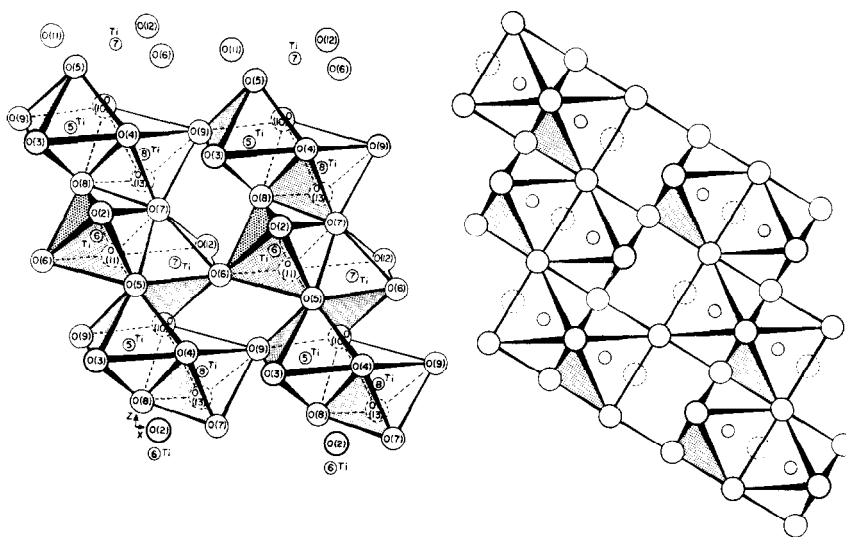


FIG. 2(a). An illustration of the manner in which the rutile blocks join together in $Ti_4O_7$.

(b) An idealized corundum structure projected on a plane perpendicular to the [110] direction.
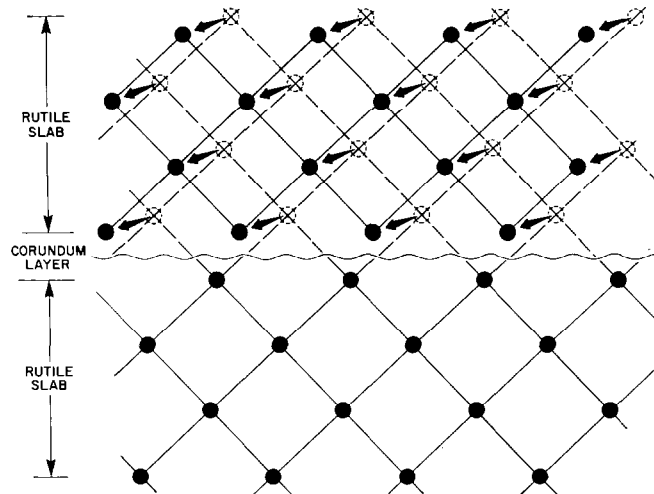
FIG. 3. A projection of the $Ti_4O_7$ structure similar to Fig. 1 with oxygen atoms excluded. Taking the origin on an empty rutile site, the relative shift of titanium atoms is from $(0,0,0)$ to $(1/2,0,1/2)$ in the rutile structure.
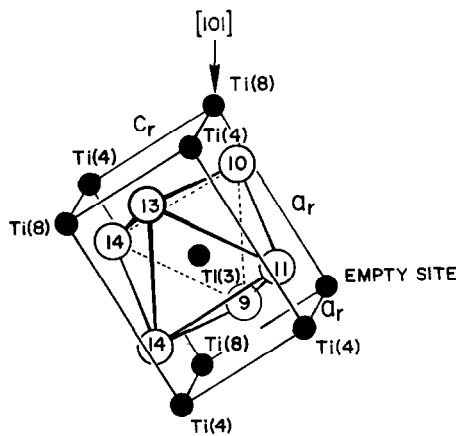


FIG. 4. A rutile unit cell is depicted with the atom identifications consistent with those of Fig. 1. A portion of the rutile layer will be observed when this cell is viewed down the [101] direction.

the octahedra share faces, edges, and corners, resembling the corundum arrangement. In the rutile structure each titanium atom has ten nearest titanium neighbors, two at 2.958 Å across a shared edge and eight at 3.549 Å across a shared corner (16). In $Ti_4O_7$, each titanium atom has 11 nearest titanium neighbors. Ti(1) through Ti(4), which are inside a rutile block, have the same type of environment. They each have nine neighbors within the same block and two from an adjacent block. Ti(5) through Ti(8), which are at the ends of the rutile blocks, have six nearest neighbors from the same block and five from the adjacent block. Within the rutile blocks the average Ti–Ti distances across a shared octahedral edge and corner are 2.972 and 3.576 Å, respectively. As can be seen these distances in $TiO_2$ are slightly shorter. Between rutile blocks the average Ti–Ti distances across the shared octahedral face and edge are 2.815 and 3.149 Å, respectively. These equivalent

TABLE II

Ti-OCTAHEDRA[a]

| Ti(1)–O(1) | 1.964 | $e^{1/1b}$ | O(1)–O(1) | 2.620 | | O(4)–O(6) | 2.797 |
|---|---|---|---|---|---|---|---|
| –O(1) | 1.940 | | O(1)–O(2) | 2.892 | | O(4)–O(2) | 3.001 |
| –O(2) | 1.931 | | O(1)–O(4) | 3.095 | | O(5)–O(1) | 2.945 |
| –O(4) | 2.058 | | O(1)–O(6) | 2.864 | | O(5)–O(2) | 2.885 |
| –O(5) | 2.107 | | O(1)–O(2) | 2.781 | $e^{1/5}$ | O(5)–O(4) | 2.691 |
| –O(6) | 2.070 | | O(1)–O(6) | 2.731 | $e^{1/7}$ | O(5)–O(6) | 2.711 |
| Average | 2.012 | | | 2.834 | | | |

TABLE II—*continued*

| Ti–O | dist. | | O–O | dist. | | O–O | dist. |
|---|---|---|---|---|---|---|---|
| Ti(2)–O(1) | 1.935 | | O(3)–O(1) | 2.818 | | O(4)–O(2) | 2.820 |
| –O(2) | 1.992 | | O(3)–O(2) | 2.890 | | O(4)–O(3) | 2.922 |
| –O(3) | 2.051 | $e^{2/2}$ | O(3)–O(3) | 2.687 | | O(7)–O(1) | 2.859 |
| –O(3) | 1.937 | | O(3)–O(4) | 2.942 | $e^{2/6}$ | O(7)–O(2) | 2.767 |
| –O(4) | 2.081 | | O(1)–O(2) | 2.875 | | O(7)–O(3) | 3.059 |
| –O(7) | 2.092 | | O(2)–O(3) | 2.778 | $e^{2/8}$ | O(7)–O(4) | 2.742 |
| Average | 2.015 | | | 2.847 | | | |
| Ti(3)–O(9) | 2.077 | $e^{3/5}$ | O(10)–O(9) | 2.688 | | O(13)–O(11) | 2.977 |
| –O(10) | 2.041 | $e^{3/7}$ | O(10)–O(11) | 2.708 | | O(13)–O(14) | 2.803 |
| –O(11) | 2.030 | | O(10)–O(13) | 2.893 | | O(14)–O(9) | 2.807 |
| –O(13) | 1.946 | | O(10)–O(14) | 2.899 | | O(14)–O(11) | 3.006 |
| –O(14) | 1.997 | | O(9)–O(11) | 2.835 | | O(14)–O(13) | 2.911 |
| –O(14) | 1.946 | | O(9)–O(14) | 2.746 | $e^{3/3}$ | O(14)–O(14) | 2.671 |
| Average | 2.006 | | | 2.829 | | | |
| Ti(4)–O(8) | 2.032 | $e^{4/6}$ | O(8)–O(11) | 2.674 | | O(14)–O(12) | 2.781 |
| –O(10) | 2.052 | | O(8)–O(12) | 2.893 | | O(14)–O(13) | 2.966 |
| –O(12) | 1.979 | $e^{4/8}$ | O(8)–O(13) | 2.737 | | O(12)–O(11) | 2.994 |
| –O(12) | 2.019 | | O(8)–O(14) | 2.883 | | O(12)–O(12) | 2.707 |
| –O(13) | 2.008 | | O(11)–O(12) | 2.769 | $e^{4/4}$ | O(12)–O(13) | 3.012 |
| –O(14) | 1.931 | | O(11)–O(13) | 2.782 | | O(12)–O(14) | 2.797 |
| Average | 2.004 | | | 2.833 | | | |
| Ti(5)–O(3) | 1.867 | | O(4)–O(3) | 2.951 | $e^{5/7}$ | O(10)–O(5) | 2.603 |
| –O(4) | 2.031 | $e^{1/5}$ | O(4)–O(5) | 2.691 | $f^{5/8}$ | O(10)–(O8) | 2.671 |
| –O(5) | 1.981 | $f^{5/8}$ | O(4)–O(8) | 2.698 | | O(9)–O(3) | 2.923 |
| –O(8) | 2.059 | $f^{5/8}$ | O(4)–O(10) | 2.713 | | O(9)–O(5) | 2.927 |
| –O(9) | 1.959 | | O(3)–O(5) | 2.913 | | O(9)–O(8) | 2.837 |
| –O(10) | 2.170 | | O(3)–O(8) | 3.129 | $e^{5/3}$ | O(9)–O(10) | 2.712 |
| Average | 2.011 | | | 2.814 | | | |
| Ti(6)–O(2) | 1.943 | | O(2)–O(5) | 2.850 | | O(8)–O(6) | 2.969 |
| –O(5) | 1.988 | | O(2)–O(6) | 2.998 | $e^{6/8}$ | O(8)–O(7) | 2.587 |
| –O(6) | 1.899 | $e^{2/6}$ | O(2)–O(7) | 2.767 | $f^{6/7}$ | O(11)–O(5) | 2.682 |
| –O(7) | 2.169 | | O(2)–O(8) | 2.948 | | O(11)–O(6) | 2.976 |
| –O(8) | 1.984 | | O(5)–O(6) | 3.043 | $f^{6/7}$ | O(11)–O(7) | 2.699 |
| –O(11) | 2.125 | $f^{6/7}$ | O(5)–O(7) | 2.638 | $e^{4/6}$ | O(11)–O(8) | 2.674 |
| Average | 2.018 | | | 2.819 | | | |
| Ti(7)–O(5) | 2.146 | $e^{1/7}$ | O(6)–O(5) | 2.711 | | O(12)–O(7) | 3.028 |
| –O(6) | 1.937 | | O(6)–O(7) | 2.848 | | O(12)–(O10) | 2.947 |
| –O(7) | 1.990 | | O(6)–O(10) | 2.914 | $f^{6/7}$ | O(11)–O(5) | 2.682 |
| –O(10) | 2.012 | | O(6)–O(12) | 2.833 | $f^{6/7}$ | O(11)–O(7) | 2.699 |
| –O(11) | 2.103 | | O(5)–O(10) | 2.603 | $e^{3/7}$ | O(11)–O(10) | 2.702 |
| –O(12) | 1.848 | $f^{6/7}$ | O(5)–O(7) | 2.638 | | O(11)–O(12) | 3.072 |
| Average | 2.006 | | | 2.806 | | | |
| Ti(8)–O(4) | 2.116 | $e^{2/8}$ | O(4)–O(7) | 2.742 | $f^{5/8}$ | O(10)–O(8) | 2.671 |
| –O(7) | 2.011 | $f^{5/8}$ | O(4)–O(8) | 2.698 | | O(10)–O(9) | 3.106 |
| –O(8) | 2.191 | | O(4)–O(9) | 3.033 | | O(13)–O(7) | 2.848 |
| –O(9) | 1.859 | $f^{5/8}$ | O(4)–O(10) | 2.713 | $e^{4/8}$ | O(13)–O(8) | 2.734 |
| –O(10) | 2.019 | $e^{6/8}$ | O(7)–O(8) | 2.587 | | O(13)–O(9) | 2.918 |
| –O(13) | 1.938 | | O(7)–O(9) | 2.933 | | O(13)–O(10) | 2.892 |
| Average | 2.022 | | | 2.823 | | | |

[a] All the standard deviations for Ti–O distances are less than 0.004 Å while those of O–O distances are less than 0.005 Å.

[b] $e^{1/1}$ or $f^{5/8}$ next to an O–O distance indicate that the distance is either a shared edge or part of a shared face, between Ti(1)–Ti(1) and Ti(5)–Ti(8), respectively.

| | Average | | | | Average |
|---|---|---|---|---|---|
| O(1)–Ti(1) | 1.964 | 1.946 | O(8)–Ti(4) | 2.032 | 2.067 |
| –Ti(1) | 1.940 | | –Ti(5) | 2.059 | |
| –Ti(2) | 1.935 | | –Ti(6) | 1.984 | |
| | | | –Ti(8) | 2.191 | |
| O(2)–Ti(1) | 1.931 | 1.955 | O(9)–Ti(3) | 2.077 | 1.965 |
| –Ti(2) | 1.992 | | –Ti(5) | 1.959 | |
| –Ti(6) | 1.943 | | –Ti(8) | 1.859 | |
| O(3)–Ti(2) | 2.051 | 1.952 | O(10)–Ti(3) | 2.041 | 2.061 |
| –Ti(2) | 1.937 | | –Ti(5) | 2.170 | |
| –Ti(5) | 1.867 | | –Ti(7) | 2.012 | |
| | | | –Ti(8) | 2.019 | |
| O(4)–Ti(1) | 2.058 | 2.072 | O(11)–Ti(3) | 2.030 | 2.078 |
| –Ti(2) | 2.081 | | –Ti(4) | 2.052 | |
| –Ti(5) | 2.031 | | –Ti(6) | 2.125 | |
| –Ti(8) | 2.116 | | –Ti(7) | 2.103 | |
| O(5)–Ti(1) | 2.107 | 2.056 | O(12)–Ti(4) | 1.979 | 1.949 |
| –Ti(5) | 1.981 | | –Ti(4) | 2.019 | |
| –Ti(6) | 1.988 | | –Ti(7) | 1.848 | |
| –Ti(7) | 2.146 | | | | |
| O(6)–Ti(1) | 2.070 | 1.969 | O(13)–Ti(3) | 1.946 | 1.964 |
| –Ti(6) | 1.899 | | –Ti(4) | 2.008 | |
| –Ti(7) | 1.937 | | –Ti(8) | 1.938 | |
| O(7)–Ti(2) | 2.092 | 2.066 | O(14)–Ti(3) | 1.997 | 1.958 |
| –Ti(6) | 2.169 | | –Ti(3) | 1.946 | |
| –Ti(7) | 1.990 | | –Ti(4) | 1.931 | |
| –Ti(8) | 2.011 | | | | |

distances in $Ti_2O_3$ have been reported as 2.592 and 2.990 Å (17). From a comparison of these latter distances it would appear that the corundum-like layers in $Ti_4O_7$ are quite distorted relative to $Ti_2O_3$ and the rutile blocks are only slightly distorted relative to $TiO_2$ on the average.

It can be seen from Table III that eight oxygen atoms have coordination number three, while the remaining six have coordination number four. All of the four coordinated oxygens and two of the three-coordinated ones, O(6) and O(9), are shared between rutile blocks, while each of the six remaining three-coordinated oxygens belong only to one rutile block. The average Ti–O distances for the three- and four-coordinated oxygen atoms are 1.957 and 2.067 Å, respectively. These observed values are in remarkably good agreement with those calculated from the Shannon and Prewitt radii (18) (1.97 and 2.05 Å, respectively), assuming that the Ti atoms

bonded to the three-coordinated oxygens have a charge 4+ and the Ti atoms bonded to the four-coordinated oxygens have a charge 3+. On the other hand, as can be seen in Table II the average values of the Ti–O distances for each octahedron range from 2.004 to 2.022 Å, which indicates that the $Ti^{3+}$ and $Ti^{4+}$ atoms are not ordered. The difference between $O - 3Ti = 1.957$ and $O - 4Ti = 2.067$ could be a coordination effect. An indication of the distortion of an oxygen octahedron is measured by the standard deviation calculated from the average Ti–O distance for the given octahedron. In general an octahedron at the end of a rutile block has a standard deviation twice that of an octahedron within a rutile block. It should be pointed out that for each octahedron within a rutile block there are three short Ti–O distances and three long ones, whereas for each octahedron at the end of a rutile block the difference is not as clear.

It is of interest to note that as one proceeds along the homologous series in the direction $TiO_2 \rightarrow Ti_2O_3$, the thickness of the rutile slabs in terms of $n$ octahedra is diminishing until an apparent limit of $n = 3$ is reached for $Ti_3O_5$. The structure of the low temperature phase of $Ti_3O_5$ has been reported as monoclinic, space group $C\ 2/m$ with unit cell dimensions (5):

$$a = 9.752\ \text{Å},$$
$$b = 3.802\ \text{Å},$$
$$c = 9.442\ \text{Å},$$
$$\beta = 91.55°.$$

The X-ray density of this compound is nearly identical to that of rutile, 4.25 g/cm³, and quite far below that of $Ti_2O_3$ which is 4.57 g/cm³. It would seem from these data that $Ti_3O_5$ may actually be a low-pressure phase in which case this compound is of considerable interest for future high-pressure studies.

## Conclusion

The $Ti_4O_7$ structure consists of rutile-like slabs of $TiO_6$ octahedra extending indefinitely in the a–b plane and four octahedra thick along the c axis. The sharing of octahedral faces, edges, and corners between rutile blocks is similar to that which occurs in the corundum structure. In general, the relative distortion of the oxygen octahedra is greater within the corundum-like layers than within the rutile blocks. The average Ti–Ti distances within a rutile block are 2.972 and 3.576 Å across a shared octahedral edge and corner, respectively, as compared

## TABLE IV

### Ti–Ti Distances (Å)

| | | | | | | | | |
|---|---|---|---|---|---|---|---|---|
| Ti(1)–Ti(1) | edge[a] | 2.895 | Ti(3)–Ti(8) | corner[a] | 3.799 | Ti(6)–Ti(1) | corner[a] | 3.428 |
| –Ti(5) | edge[a] | 3.026 | –Ti(5) | edge[b] | 3.113 | –Ti(5) | corner[a] | 3.560 |
| –Ti(2) | corner[a] | 3.611 | –Ti(6) | corner[b] | 3.808 | –Ti(5) | corner[a] | 3.573 |
| –Ti(2) | corner[a] | 3.507 | | | | –Ti(7) | face[b] | 2.813 |
| –Ti(2) | corner[a] | 3.560 | Ti(4)–Ti(4) | edge[a] | 2.942 | –Ti(7) | corner[b] | 3.424 |
| –Ti(2) | corner[a] | 3.574 | –Ti(8) | edge[a] | 3.026 | –Ti(8) | edge[b] | 3.285 |
| –Ti(6) | corner[a] | 3.535 | –Ti(3) | corner[a] | 3.579 | –Ti(4) | edge[b] | 3.072 |
| –Ti(6) | corner[a] | 3.795 | –Ti(3) | corner[a] | 3.607 | –Ti(3) | corner[b] | 3.808 |
| –Ti(6) | corner[a] | 3.428 | –Ti(3) | corner[a] | 3.507 | | | |
| –Ti(7) | edge[b] | 3.114 | –Ti(3) | corner[a] | 3.555 | Ti(7)–Ti(4) | corner[a] | 3.464 |
| –Ti(8) | corner[b] | 3.808 | –Ti(7) | corner[a] | 3.464 | –Ti(4) | corner[a] | 3.755 |
| | | | –Ti(7) | corner[a] | 3.755 | –Ti(4) | corner[a] | 3.543 |
| Ti(2)–Ti(2) | edge[a] | 2.948 | –Ti(7) | corner[a] | 3.543 | –Ti(3) | edge[a] | 3.021 |
| –Ti(6) | edge[a] | 3.019 | –Ti(6) | edge[b] | 3.072 | –Ti(8) | corner[a] | 3.559 |
| –Ti(1) | corner[a] | 3.611 | –Ti(5) | corner[b] | 3.791 | –Ti(8) | corner[a] | 3.575 |
| –Ti(1) | corner[a] | 3.507 | | | | –Ti(6) | face[b] | 2.813 |
| –Ti(1) | corner[a] | 3.560 | | | | –Ti(6) | corner[b] | 3.424 |
| –Ti(1) | corner[a] | 3.574 | Ti(5)–Ti(1) | edge[a] | 3.026 | –Ti(5) | edge[b] | 3.242 |
| –Ti(5) | corner[a] | 3.756 | –Ti(2) | corner[a] | 3.756 | –Ti(1) | edge[b] | 3.114 |
| –Ti(5) | corner[a] | 3.542 | –Ti(2) | corner[a] | 3.542 | –Ti(2) | corner[b] | 3.789 |
| –Ti(5) | corner[a] | 3.470 | –Ti(2) | corner[a] | 3.470 | | | |
| –Ti(8) | edge[b] | 3.069 | –Ti(6) | corner[a] | 3.560 | Ti(8)–Ti(3) | corner[a] | 3.426 |
| –Ti(7) | corner[b] | 3.789 | –Ti(6) | corner[a] | 3.573 | –Ti(3) | corner[a] | 3.534 |
| | | | –Ti(8) | face[b] | 2.816 | –Ti(3) | corner[a] | 3.799 |
| Ti(3)–Ti(3) | edge[a] | 2.901 | –Ti(8) | corner[b] | 3.418 | –Ti(4) | edge[a] | 3.026 |
| –Ti(7) | edge[a] | 3.021 | –Ti(7) | edge[b] | 3.242 | –Ti(7) | corner[a] | 3.559 |
| –Ti(4) | corner[a] | 3.579 | –Ti(3) | edge[b] | 3.113 | –Ti(7) | corner[a] | 3.575 |
| –Ti(4) | corner[a] | 3.607 | –Ti(4) | corner[b] | 3.791 | –Ti(5) | face[b] | 2.816 |
| –Ti(4) | corner[a] | 3.507 | | | | –Ti(5) | corner[b] | 3.418 |
| –Ti(4) | corner[a] | 3.555 | Ti(6)–Ti(2) | edge[a] | 3.019 | –Ti(6) | edge[b] | 3.285 |
| –Ti(8) | corner[a] | 3.426 | –Ti(1) | corner[a] | 3.535 | –Ti(2) | edge[b] | 3.069 |
| –Ti(8) | corner[a] | 3.534 | –Ti(1) | corner[a] | 3.795 | –Ti(1) | corner[b] | 3.808 |

[a] All labelled $a$ represent inside the rutile block.
[b] All labelled $b$ represent between the rutile block.

to 2.958 and 3.549 Å in the rutile structure. The average Ti–Ti distances across a shared face and edge in the corundum layers are 2.815 and 3.149 Å, respectively, as compared to 2.592 and 2.990 Å in the corundum structure. It would appear that the predominant symmetry of the $Ti_4O_7$ substructure is that of rutile rather than corundum and the distortion of oxygen octahedra and average Ti–Ti distances reflect this.

## Acknowledgments

## References

1. S. ANDERSSON AND A. MAGNÉLI, Naturwissenschaften 43, 495 (1956).
2. S. ANDERSSON, B. COLLIN, U. KUYLENSTIERNA, AND A. MAGNÉLI, Acta Chem. Scand. 11, 1641 (1957).
3. S. ANDERSSON, "XVIᵉ Congres International de Chimie Pure et Appliquee," Paris, 1957.
4. S. ANDERSSON AND L. JAHNBERG, Arkiv Kemi 21, 413 (1963).
5. S. ÅSBRINK AND A. MAGNÉLI, Acta Crystallogr. 12, 575 (1959).
6. R. F. BARTHOLOMEW AND D. R. FRANKL, Phys. Rev. 187, 828 (1969).
7. M. MAREZIO, P. D. DERNIER, D. B. McWHAN, AND J. P. REMEIKA, Mater. Res. Bull. (in press).
8. R. F. BARTHOLOMEW AND W. B. WHITE, J. Cryst. Growth 6, 249 (1970).
9. A. SANTORO AND A. D. MIGHELL, Acta Crystallogr. Sect. A 26, 124 (1970).

*10.* C. J. FRITCHIE, unpublished computer program for Fourier synthesis (1967).

*11.* W. R. BUSING, K. O. MARTIN, AND H. A. LEVY, Oak Ridge National Laboratory Report TM-306.

*12.* D. T. CROMER AND J. T. WABER, *Acta Crystallogr.* **18**, 104 (1965).

*13.* D. T. CROMER, *Acta Crystallogr.* **18**, 17 (1965).

*14.* C. T. PREWITT, unpublished computer program for crystallographic least-squares refinement (1966).

*15.* W. R. BUSING AND H. A. LEVY, ORNL Report 59-12-3 (1959).

*16.* S. C. ABRAHAMS AND J. L. BERNSTEIN, to be published.

*17.* S. C. ABRAHAMS, *Phys. Rev.* **130**, 2230 (1963).

*18.* R. D. SHANNON AND C. T. PREWITT, *Acta Crystallogr. Sect. B* **25**, 925 (1969).